ELSEVIER

Sensors and Actuators B 49 (1998) 93–100

SENSORS AND ACTUATORS B CHEMICAL

A first principles model of metal oxide gas sensors for measuring combustibles

A.D. Brailsford, M. Yussouff, E.M. Logothetis *

Ford Motor Company Research Laboratory, Physics Department, Mail Drop 3028, PO Box 2053, Dearborn, MI 48121-2053, USA

Received 12 August 1997; accepted 8 December 1997

Abstract

A first principles model is described for the operation of electrochemical type sensors designed to measure combustibles in air. It is based on the general principles presented in previous publications (A.D. Brailsford, E.M. Logothetis, Sens. Actuators, 7 (1985) 39–67; A.D. Brailsford, M. Yussouff, E.M. Logothetis, Sens. Actuators, B 13 (1993) 135–138; A.D. Brailsford, M. Yussouff, E.M. Logothetis, M. Shane, Sens. Actuators, B 24–25 (1995) 362–365; A.D. Brailsford, M. Yussouff, E.M. Logothetis, Sens. Actuators B 34 (1996) 407–411; and A.D. Brailsford, M. Yussouff, E.M. Logothetis, Sens. Actuators, B 35–36 (1996) 392–397) for an ab initio model developed to describe the operation of metal oxide oxygen sensors. The authors show that the e.m.f. of the combustibles sensor may be written as the difference between the e.m.f.s of two non-identical air-referenced oxygen sensors. This helps in the qualitative understanding of the observed and predicted responses of the combustibles sensors. The present model is used to analyze experimental data reported in the literature (H. Okamoto, H. Obayashi, T. Kudo, Solid State Ion. 1 (1980) 319–326; and A. Vogel, G. Baier, V. Schuele, Sens. Actuators B 15 (1993) 147–150) and to indicate the variety of behavior expected from these sensors depending on the properties of the electrode materials. This analysis is expected to aid the design and optimization of these sensors.

Keywords: Gas sensors; Combustibles; Zirconia

1. Introduction

Extensive research and development efforts have been put into the fabrication of metal oxide sensors designed to measure combustibles. The capability of measuring very small amounts of combustible gases and of operating without degradation at the harsh environment of flue gases of combustion processes are some of the desirable features of such devices. However, the sensors developed so far suffer from several problems including lack of selectivity, stability and sensitivity and long response times. It is clear that major improvements in the characteristics of these sensors require a better understanding of the fundamental processes involved in sensor operation. In this respect, the development of the underlying theory will undoubtedly aid this effort and the present work is directed towards this goal.

In previous publications [1–5], the authors developed a first principles model for describing the observed steady state responses of metal oxide oxygen sensors. This model, referred to as the BYL (Brailsford, Yussouff and Logothetis) model in the rest of this paper, is now firmly established for the commercial oxygen sensors. It has also been very successful in predicting the behavior of such sensors when the characteristics of the electrodes are varied. Here the authors use the same general principles as in the BYL development to construct a model that applies to the electrochemical (e.g. zirconia) type sensors designed to measure combustibles in air, for example, the device schematically shown in Fig. 1. The corresponding version of this model for resistive (e.g. SnO_2) type sensors will be reported in the future.

The BYL model describes the physical and chemical processes that lead to the generation of e.m.f. in an oxygen sensor. In the steady state, the equations for transport, adsorption, desorption and reactions of various species and the equation(s) for the electrochemical

* Corresponding author. Tel.: +1 313 3238553; fax: +1 313 3227044.

0925-4005/98/$19.00
PII S0925-4005(98)00093-8

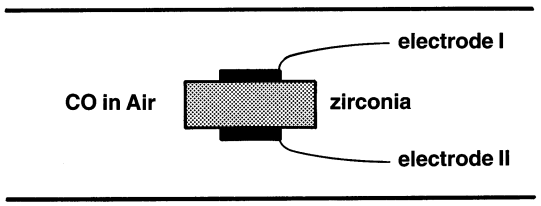

Fig. 1. Schematic of a Combustibles Sensor.

reaction between these species and zirconia, can be combined to yield a basic equation whose solution determines the concentrations of adsorbed species on the electrodes. Solving the electrostatic problem, these concentrations are then used to compute the e.m.f. of the oxygen sensor. In most of the previous publications [1–4], it was assumed that the electrochemical reaction between adsorbed oxygen atoms and oxygen vacancies in zirconia is the only reaction that produces the e.m.f. in oxygen sensors. It turns out that in the case of combustibles sensors, this electrochemical reaction does not suffice to yield agreement with available experimental data [6,7]. A second electrochemical reaction involving adsorbed CO and the oxygen ions of zirconia [5] must also be included in the computation of the e.m.f. of the combustibles sensor to get agreement with the experimental results. The present model, based on two electrochemical reactions, can also predict a variety of behavior expected from these combustibles sensors when the properties of the electrode materials are varied.

2. Electrochemical gas sensor

Fig. 1 shows schematically an electrochemical gas sensor with a metal oxide electrolyte ceramic, such as yttria stabilized zirconia (ZrO_2), placed between two electrodes. If the two electrodes are dissimilar, this device acts as a combustibles sensor when placed in an enclosure with both of its electrodes exposed to the same measurement gas consisting of air mixed with a combustible gas. If the enclosure is divided into two chambers as shown in Fig. 2 and one electrode is exposed to a reference gas atmosphere, say air, while the other is exposed to the given measurement gas, the device can generate an e.m.f. even when the two electrodes are similar. The configuration of Fig. 2 is similar to that of

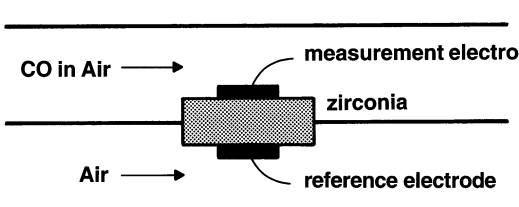

Fig. 2. Schematic of an Oxygen Sensor.

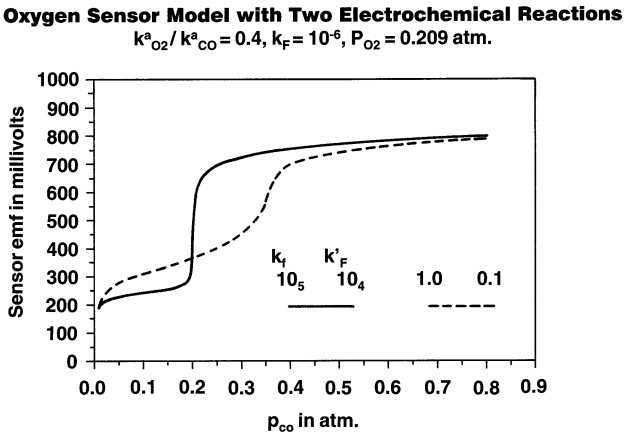

Fig. 3. Computed sensor e.m.f. at 650°C for different k_f and k'_F.

ZrO_2 oxygen sensors. The commercial automotive oxygen gas sensor which is used for monitoring the exhaust gas from internal combustion engines is generally thimble shaped and its inner electrode is exposed to air. Here (and throughout this paper), the authors assume the measurement gas to be a mixture of the combustible gas CO and air. A similar analysis can be used for other combustibles like H_2, CH_4 etc. Two examples of the e.m.f. of the device of Fig. 2 as a function of P_{CO} (the partial pressure of CO), are depicted in Fig. 3. These are theoretical curves computed from the BYL model of automotive oxygen sensors. The e.m.f. output of a typical automotive ZrO_2 oxygen sensor is like the solid curve in Fig. 3, i.e. it is small for low values of P_{CO} and high for large values of P_{CO}, with a step-like transition at the 'switch-point' value of P_{CO} that is generally close to the stoichiometric composition of the measurement gas mixture for CO oxidation.

The authors first review the salient features of the BYL model for the oxygen sensor and then present the model for the combustibles sensor depicted in Fig. 1. In the case of the oxygen sensor shown in Fig. 2, only oxygen molecules diffuse to the air-reference electrode and get adsorbed or desorbed. Both CO and O_2 molecules diffuse to the surface of the measurement electrode where they may adsorb, desorb and also react. Products of the reaction (e.g. CO_2) may also desorb. The reactions taking place on the measurement electrode surface may be written as follows [1–4]:

$$O_{2g} + \Sigma \underset{k_1^d}{\overset{k_1^a}{<----->}} O_{2ads},$$

$$CO_g + \Sigma \underset{k_2^d}{\overset{k_2^a}{<----->}} CO_{ads},$$

$$CO_{2g} + \Sigma \underset{k_3^d}{\overset{k_3^a}{<----->}} CO_{2ads},$$

$$O_{2ads} + \Sigma \underset{k_R}{\overset{k_D}{<\!-\!-\!-\!-\!->}} 2O_{ads},$$

$$CO_{ads} + O_{ads} \underset{k_b}{\overset{k_f}{<\!-\!-\!-\!-\!->}} CO_{2ads} + \Sigma \quad (1)$$

where Σ denotes a vacant surface site on the electrode. By detailed balance [1–4], rate constants are related to the equilibrium constant [8], K_C, for the oxidation of CO at the absolute temperature T of the sensor:

$$K_C = \exp[33906/T - 10.4192]$$
$$= [k_f k_2^a k_3^d (2k_1^a k_D)^{1/2}]/[k_b k_2^d k_3^a (k_1^d k_R)^{1/2}] \quad (2)$$

Since the equilibrium constant is known at a given temperature, this equation may be used to determine one of the rate constants, say k_b, when all other rate constants are specified.

The concentrations of the species O_{ads}, O_{2ads}, CO_{ads} and $CO_{2\ ads}$ on the surface of the electrode are denoted by θ_α, $\alpha = O$, O_2, CO or CO_2, respectively. Let the number of sites on the electrode surface accessible to all the adsorbed species be ω per unit area and let (dn_α/dt) be the rate of change of the number of particles of the species α. This change, due to the adsorption /desorption described above, can be written as [1–4]

$$(dn_\alpha/dt)/\omega = k_\alpha^a P_\alpha^{(0)} - k_\alpha^d \theta_\alpha \quad (3)$$

where $P_\alpha^{(0)}$ are partial pressures at the electrode as opposed to the given partial pressures P_α far away from the electrodes. In general, $P_\alpha^{(0)}$ is different from P_α except when the entire system (gases + device) is in thermodynamic equilibrium. Since mass transport of the gases to the electrode is responsible for the partial pressure differences, one can also write

$$(dn_\alpha/dt)/\omega = \kappa D_\alpha (P_\alpha - P_\alpha^{(0)})/D_{O_2} \quad (4)$$

where D_α, $\alpha = O_2$, CO and CO_2 are the diffusion coefficients of these gases (through nitrogen) respectively. The mass transfer coefficient κ depends upon temperature and the detailed characteristics of the diffusional transfer of molecules from the bulk of the gas to the surface of the electrode.

The electrochemical reactions take place at the triple lines on the surface where the porous electrode, zirconia and the gases meet each other. One such reaction is between adsorbed oxygen and oxygen vacancies, another reaction is between adsorbed CO and oxygen ions of the ZrO_2 electrolyte. In both reactions, electrons are transferred from or to the electrodes. Thus, the authors consider two electrochemical reactions:

$$O_{ads} + v_O^{2+} + 2e^-(\text{electrode}) \underset{k_F}{\overset{k_A}{<\!-\!-\!->}} O_O(\text{oxide}) \quad (5)$$

$$CO_{2ads} + v_O^{2+} + 2e^-(\text{electrode}) \underset{k_F'}{\overset{k_A'}{<\!-\!-\!->}} CO_{ads} + O_O(\text{oxide}) \quad (6)$$

Here v_O^{2+} denotes a doubly charged oxygen vacancy whose fractional occupation on the surface is denoted by θ_v. Again, by detailed balance [5], the rate constants k_F, k_F', k_A and k_A' are related:

$$(k_F' k_A)/(k_F k_A') = (k_f/k_b) \quad (7)$$

In the steady state, the net change in the number of electrons vanishes:

$$(dn_e/dt)/\omega = 0 = k_F - k_A \theta_v \theta_O + k_F' \theta_{CO} - k_A' \theta_v \theta_{CO2}$$

whence

$$\theta_v = (k_F + k_F' \theta_{CO})/(k_A \theta_O + k_A' \theta_{CO2}).$$

The coupled equations satisfied by θ_α are as follows:

$$(d\theta_{O2}/dt) = 0 = (dn_1/dt)/\omega - k_D \theta_{O2} + (1/2) k_R \theta_O^2$$

$$(d\theta_{CO}/dt) = 0 = (dn_2/dt)/\omega - k_f \theta_O \theta_{CO} + k_b \theta_{CO2} - k_F' \theta_{CO} + k_A' \theta_v \theta_{CO2}$$

$$(d\theta_{CO2}/dt) = 0 = (dn_3/dt)/\omega + k_f \theta_O \theta_{CO} - k_b \theta_{CO2} + k_F' \theta_{CO} - k_A' \theta_v \theta_{CO2}$$

$$(d\theta_O/dt) = 0 = 2k_D \theta_{O2} - k_R \theta_O^2 - k_f \theta_O \theta_{CO} + k_b \theta_{CO2} + k_F - k_A \theta_v \theta_O$$

All these equations, together with Eq. (3) and Eq. (4), can be manipulated algebraically to yield an equation satisfied by θ_O, the surface concentration of oxygen adatoms on the measurement electrode. Defining a variable z such that

$$\theta_O = [(2k_1^a k_D) P_{O_2}/(k_1^d k_R)]^{1/2} z \quad (8a)$$

one can write

$$\theta_{CO} = [k_2^a/k_2^d] \times [P_{CO} - 2P_{O_2}(D_{O_2}/D_{CO} + \kappa/k_2^a)(1 - z^2)] \times /\{1 + (\kappa/k_1^a)(1 + k_1^d/k_D)\}] \quad (8b)$$

where D_{O2} and D_{CO} are the diffusion coefficients of O_2 and CO in air respectively. Similar expressions for the concentrations of other species on the measurement electrode can be written down as described in detail in the previous work [5]. It can be shown [5] that z satisfies the equation:

$$(z^3 + a_2 z^2 + a_1 z + a_0)(b_2 z^2 + b_1 z + b_0) + (c_3 z^3 + c_2 z^2 + c_1 z + c_0) = 0 \quad (8c)$$

where the coefficients are functions of rate constants, temperature and partial pressures. One can solve this

basic equation and obtain the steady state values of the concentrations θ_α of adsorbed species on the measurement electrode. Solving the electrostatic problem inside the zirconia electrolyte [1–5] with appropriate boundary conditions, one gets the sensor e.m.f. in millivolts as:

$$V_0(T/23.21)\ln[\theta_v/\theta_{AIR}] \tag{9a}$$

where $\theta_{AIR} = k_F/(k_A\theta_{OAIR})$.

The sensor e.m.f. can be computed using Eq. (9a) by specifying the parameters κ, k_1^a, k_2^a, k_3^a, k_1^d, k_2^d, k_3^d, k_R, k_D, k_f, k_F and k'_F along with T, P_{O2} and P_{CO} in the measurement gas. Two typical results of this BYL model are depicted in Fig. 3. The e.m.f. versus P_{CO} curve is characterized by a low e.m.f. region and a high e.m.f. region. According to the model, the value of P_{CO} where the transition from low to high e.m.f. takes place (the so-called switch-point), is determined by the relation

$$2P_{O_2}/P_{CO} = [1 + (\kappa/k_1^a)(1 + k_1^d/k_D)]/[D_{O_2}/D_{CO} + (\kappa/k_2^a)] \tag{9b}$$

In Fig. 3, the solid curve has a sharp switch-point at a lower value of P_{CO} than the rather non-sharp transition in the dashed curve. As shown in the previous publications [1–5], within the framework of the BYL model of oxygen gas sensors, it is the lower value of the rate constant k_f that leads to a lower value of the high e.m.f. of the dashed curve. Similarly, the lower value of the rate constant k'_F leads to a higher value of the low e.m.f. of the dashed curve in Fig. 3. The ratio (k_1^a/k_2^a) is most effective in determining the switch-point.

In the case of the combustibles sensor shown in Fig. 1, there is no reference gas and the entire device is exposed to the same measurement gas. An e.m.f. will develop if and only if the two electrodes are dissimilar, which the authors here assume to be the case. The electrodes are designated as I and II. Again, the measurement gas is assumed to consist of only CO in air (and a similar analysis can be used for H_2 or CH_4 etc. in air). Note that in the case of combustibles sensor, CO and O_2 molecules diffuse to the surfaces of both the electrodes where they may adsorb, desorb or react. Products of the reaction (e.g. CO_2) may also desorb from both the electrodes. Then, processes like those described by Eq. (1) may be assumed to take place at each of the two electrodes. The corresponding rate constants are labeled by additional subscripts I (e.g. $k_{f,I}$) or II (e.g. $k_{f,II}$). By detailed balance [1–4], rate constants at each electrode are related, as in Eq. (2), to the equilibrium constant K_C. Such equations are used below to determine $k_{b,I}$ and $k_{b,II}$ on the electrodes I and II respectively after all other rate constants are specified (although in principle, any one rate constant on a given electrode can be determined when the rest of the rate constants on that electrode are specified).

The electrochemical reactions given by Eq. (5) and Eq. (6) are assumed to take place at the triple lines on the surface where the distinct porous electrodes, zirconia and the gases meet each other. The detailed balance relations, as in Eq. (7), hold between the rate constants at each electrode. The basic equations, like Eq. (8c), of the model at each electrode are solved to yield the steady state values of the concentrations of adsorbed species on the two electrodes, $\theta_{\alpha,I}$ and $\theta_{\alpha,II}$, where $\alpha = O$, O_2, CO or CO_2. Again, the electrostatic problem inside zirconia [1–5] with appropriate boundary conditions for each electrode may be solved to yield the sensor e.m.f. in millivolts as

$$V_0 = (T/23.21)\ln[\theta_{v,I}/\theta_{v,II}] \tag{10}$$

where

$$\theta_{v,I} = (k_{F,I} + k'_{F,I}\theta_{CO,I})/(k_{A,I}\theta_{O,I} + k'_{A,I}\theta_{CO2,I}), \text{ and}$$

$$\theta_{v,II} = (k_{F,II} + k'_{F,II}\theta_{CO,II})/(k_{A,II}\theta_{O,II} + k'_{A,II}\theta_{CO2,II}).$$

The sensor e.m.f. can be computed by specifying the parameters κ, k_1^a, k_2^a, k_3^a, k_1^d, k_2^d, k_3^d, k_R, k_D, k_f, k_F and k'_F at each electrode, along with T, P_{O2} and P_{CO} in the sample gas.

It is possible to relate the response of the combustibles sensor to the more familiar response of the oxygen sensor. Such a connection is not necessary, but it is helpful in understanding the response of the combustibles sensor. The authors can rewrite Eq. (10) as

$$\begin{aligned} V_0 &= (T/23.21)\ln[\theta_{v,I}/\theta_{v,II}] \\ &= (T/23.21)(\ln[\theta_{v,I}/\theta_{AIR}] - \ln[\theta_{v,II}/\theta_{AIR}]) \\ &= (V_{0,I} - V_{0,II}) \end{aligned} \tag{11}$$

where $\theta_{AIR} = k_F/(k_A\theta_{OAIR})$ (see Eq. (9a)) with an arbitrary non-zero oxygen adatom concentration θ_{OAIR}. The concentration θ_{0AIR} used here does not physically exist in the actual combustibles sensor. However, suppose there is an oxygen sensor whose reference electrode has oxygen adatom concentration θ_{0AIR} and whose measurement electrode is exactly the same as electrode I of the combustibles sensor shown in Fig. 1. Its e.m.f. for the given measurement gas mixture may be denoted by $V_{0,I}$. Similarly, consider another oxygen sensor whose reference electrode has the same oxygen adatom concentration θ_{0AIR} and whose measurement electrode is exactly identical to the electrode II of the combustibles sensor shown in Fig. 1. Its e.m.f. for the same measurement gas mixture may be denoted by $V_{0,II}$. Then, Eq. (11) suggests that the e.m.f. V_0 of the combustibles sensor is the difference $(V_{0,I} - V_{0,II})$ between the e.m.f.s of these two different fictitious oxygen sensors (which have exactly identical reference electrodes exposed to air and one of which has the measurement electrode I while the other has measurement electrode II). Eq. (11) helps in understanding the theo-

retical and experimentally observed e.m.f.s of the combustibles sensor in relation to the step-like e.m.f.s of oxygen sensors. This is especially helpful in understanding the shapes of the combustibles sensor e.m.f. when the partial pressure of CO is near the switch-points of the corresponding fictitious oxygen sensors.

3. Results

For all the computed sensor e.m.f.s presented in Fig. 4 through Fig. 8, the authors assumed, for the sake of simplicity, that the following parameters have the same values on both electrodes:

$\kappa = 0.1$, $k_1^a = 0.1$, $k_3^a = 10^{-4}$, $k_1^d = 0.1$, $k_3^d = 1.0$

$k_R = 20.0$ and $k_D = 10.0$

The authors adopt these values for want of anything better, they are the same as those used previously [1–5] to successfully predict the response of commercial oxygen gas sensors. The partial pressure of oxygen in the air is denoted by P_{O2} which has the numerical value of 0.209. The parameters k_f, k_F and k'_F and the ratio (k_1^a/k_2^a) on electrodes I and II are given different values as shown in the figures to obtain different theoretical results.

To test the model, the authors consider the data of Okamoto et al. [6] obtained for a CO sensor consisting of a zirconia electrolyte with two e-beam deposited Pt electrodes, one of the electrodes being covered with a layer prepared by impregnating Al_2O_3 with H_2PtCl_6 and then reducing it. The solid line in Fig. 4 represents the experimental result for the variation of the sensor e.m.f. with P_{CO} for very small values of P_{CO}. To fit the model to these results, the authors varied the values of (k_1^a/k_2^a), k_f, k_F and k'_F on the two electrodes until the authors obtained very good agreement with experiment, shown as dotted curve in Fig. 4. The parameter values for best fit are given in Fig. 4. It must be emphasized that if the electrochemical reaction Eq. (6) is neglected (as in some applications of the BYL model where $k'_{F,I} = 0 = k'_{F,II}$ and $k'_{A,I} = 0 = k'_{A,II}$), then no physically acceptable values of other parameters can explain the observed e.m.f. [6,7] when the combustibles sensor is exposed to very small amounts of CO in air. This conclusion may be understood in terms of the BYL model for oxygen sensors in which the low e.m.f. is almost zero for very small values of P_{CO} if the second electrochemical reaction given by Eq. (6) is not included in the model. In that case, the e.m.f. of the combustibles sensor, which is the difference between two such vanishingly small e.m.f.s (see Eq. (11)) would also be vanishingly small. An additional constraint, as shown in the earlier work [5], is that the electrochemical reaction Eq. (6) has very little effect on the e.m.f. when the value of k_f is large compared with k_F and k'_F. Such large values of k_f are associated with the so called highly catalytic electrodes. On the other hand, for partially catalytic electrodes with comparatively small values of k_f, the parameters k_F and k'_F can have significant effects on the sensor e.m.f.. All these constraints restrict the choice of the parameter values of the model.

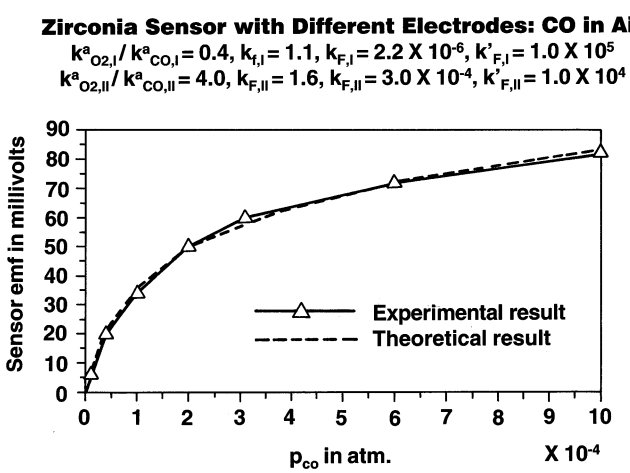

Fig. 4. Measured and computed sensor e.m.f. at 300°C.

It is noteworthy that the present model enables one to derive an analytical expression for the e.m.f. of the combustibles sensor at very small values of P_{CO}, albeit the algebra involved is somewhat lengthy. For the parameter values chosen for Fig. 4, it can be shown that Eq. (10) reduces to the approximate form

$$V_0 = (T/23.21) \times \ln[\{1 + (k'_{F,I}/k_{F,I})\theta_{CO,I}\}/\{1 + (k'_{F,II}/k_{F,II})\theta_{CO,II}\}]$$

Eq. (8b) can be used to evaluate the concentrations $\theta_{CO,I}$ and $\theta_{CO,II}$ on the two electrodes:

$$\theta_{CO} = [k_2^a/k_2^d] \times [P_{CO} - 2P_{O2}(D_{O2}/D_{CO} + \kappa/k_2^a)(1 - z^2) \times /\{1 + (\kappa/k_1^a)(1 + k_1^d/k_D)\}],$$

where z satisfies Eq. (8c). For very small values of P_{CO}, the variable z is close to but slightly less than 1.0 [3,5]. For the parameter values chosen in Fig. 4, the coefficients $a_0 \cong -a_2$, $b_0 \cong -b_2$ and $c_0 \cong -c_2$ in Eq. (8c). Furthermore, the coefficient c_2 is of the order of 10^{-14}, b_2 is of the order of 10^{-9}; a_2, a_1 and b_1 are of the order of 1.0 and the largest coefficients are c_3 and c_1 $(= c_3 a_1)$ which are of the order of 10^5. Neglecting the small coefficients, Eq. (8c) reduces to an approximate fourth order equation:

$$b_1 z^4 + c_3 z^3 - b_1 z^2 + c_3 a_1 z \cong 0,$$

where $a_1 = [P_{CO}/2P_{O2}]\ [1 + (\kappa\ /k_1^a)(1 + k_1^d/k_D)]/[D_{O2}/D_{CO} + (\kappa/k_2^a)] - 1$, $c_3 = (k'_F/k_f)$ and $b_1 = [P_{O2}(2k_1^a k_D)/(k_1^d k_R)]^{1/2}$. Factoring out $(c_3 z)$, one gets the approximate cubic equation

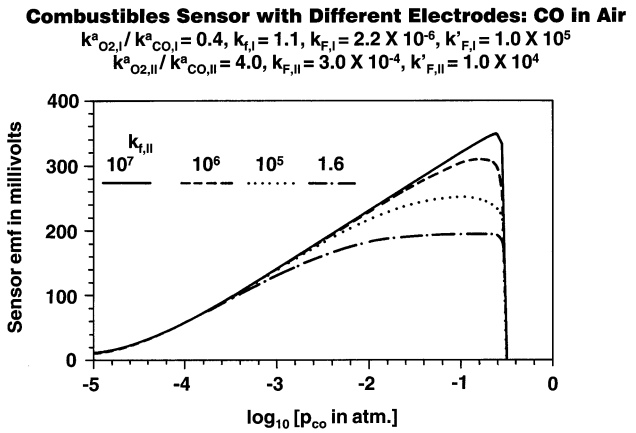

Fig. 5. Computed sensor e.m.f. at 650°C for different $k_{f,II}$.

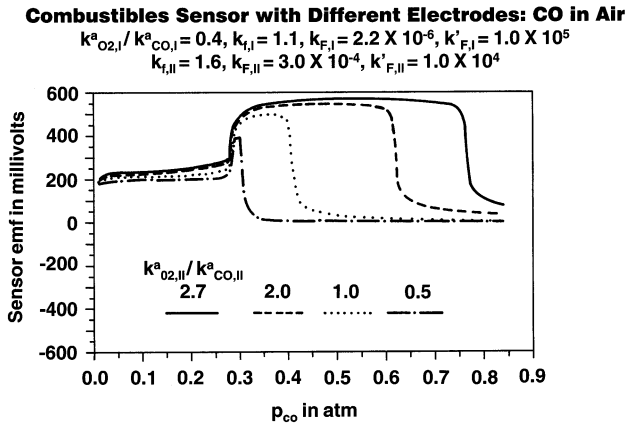

Fig. 6. Computed sensor e.m.f. at 650°C for different $k^a_{O2,II}/k^a_{CO,II}$.

$$(b_1/c_3)z^3 + z^2 - (b_1/c_3)z + a_1 \cong 0.$$

The solution for z is close (but never exactly equal) to 1. Writing $z = (1-\delta)$ where $\delta << 1$ and retaining linear terms of δ in the above equation, one obtains,

$$\delta \cong [1 + a_1]/[2(\{1 + (b_1/c_3)\}].$$

Then, the second term, $[2P_{O2}(D_{O2}/D_{CO} + \kappa/k^a_2)(1-z^2)/\{1 + (\kappa/k^a_1)(1 + k^d_1/k_D)\}]$, in the expression for θ_{CO} becomes approximately equal to $P_{CO}/(1 + b_1/c_3)$. It follows that for very small values of P_{CO}, $\theta_{CO} \cong [k^a_2/k^d_2][P_{CO}(b_1/c_3)]$. This approximate form of θ_{CO} may be substituted in Eq. (10) to obtain the dependence of e.m.f. on P_{CO} for very small values of P_{CO}:

$$V_0 = (T/23.21)\ln[(1 + B_I P_{CO})/(1 + B_{II} P_{CO})] \qquad (13)$$

where $B_I = (k^a_{2,I}/k^d_{2,I})(k_{f,I}/k_{F,I})[P_{O2}(2k^a_{1,I}k_{D,I})/(k^d_{1,I}k_{R,I})]^{1/2}$

and $B_{II} = (k^a_{2,II}/k^d_{2,II})\ (k_{f,II}/k_{F,II})$
$\times [P_{O2}(2k^a_{1,II}k_{D,II})/(k^d_{1,II}k_{R,II})]^{1/2}$

Thus, according to the approximate expressions derived from the present model, the experimental and theoretical curves shown in Fig. 4 should be described by Eq. (13) for very small values of P_{CO}. Using the rate constants appropriate for Fig. 4, one gets $B_I = 228500$ and $B_{II} = 2437$. Using these values, Eq. (13) gives e.m.f. values (not shown in Fig. 4) within 10% of the observed values shown in Fig. 4. A curve fitting procedure using the functional form of Eq. (13), however, gives an excellent fit (not shown) to the curves depicted in Fig. 4 for the numerical values $B_I = 35250$ and $B_{II} = 310$. In the limit of vanishingly small P_{CO} ($< 0.3 \times 10^{-4}$), Eq. (13) shows that the e.m.f. will be linear in P_{CO}, i.e. $V_0 \cong (T/23.21)(B_I - B_{II})P_{CO}$.

The present model can also be used to predict the response of combustibles sensors if the characteristics (e.g. rate constants for various processes) of the electrodes are changed. Fig. 5, Fig. 6, Fig. 7 and Fig. 8 provide some illustrative examples. It was stated earlier that the reaction rate constant k_f determines the high e.m.f. of the oxygen sensor. Assigning different values of k_f on electrodes I and II of the combustibles sensor amounts to the subtraction of the e.m.f.s of two oxygen sensors whose high e.m.f. values are different. As an example, the authors consider the responses when the rate constant k_f for oxidation of CO is varied on one of the electrodes. Suppose electrode I is partially catalytic with $k_{f,I} = 1.1$. When the rate constant $k_{f,II}$ for oxidation of CO on electrode II is varied, one obtains the sensor responses depicted in Fig. 5. For all values of $k_{f,II}$, the e.m.f. abruptly drops to zero for a value of P_{CO} close to stoichiometry that corresponds to the switch-point in the case of commercial oxygen sensors. For very small values (< 0.001) of P_{CO}, there is no change in the e.m.f. as $k_{f,II}$ increases. But for larger values of P_{CO}, the e.m.f. is larger for larger values of $k_{f,II}$ and saturates for $k_{f,II} = 10^7$. Similar trends are observed as $k_{f,II}$ decreases. For very small values (< 0.001) of P_{CO}, there is again no change in the e.m.f. as $k_{f,II}$ decreases. But for larger values of P_{CO}, the e.m.f. is smaller for smaller values of $k_{f,II}$ and saturates for $k_{f,II} = 1.6$ as $k_{f,II}$ is decreased further (so that for larger values of P_{CO},

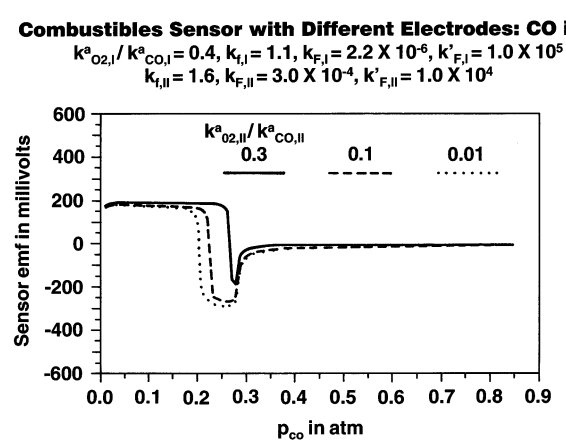

Fig. 7. Computed sensor e.m.f. at 650°C for different $k^a_{O2,II}/k^a_{CO,II}$.

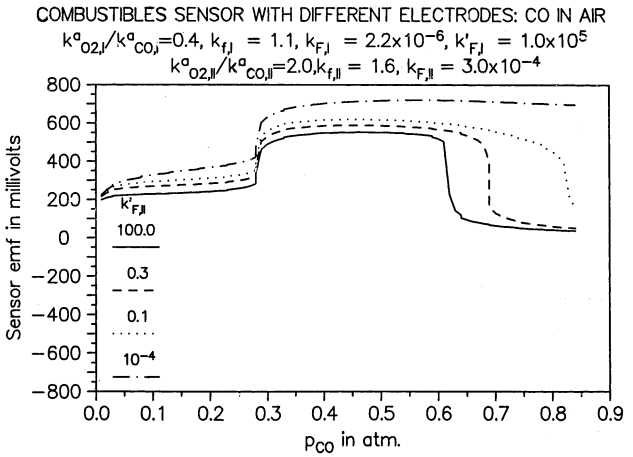

Fig. 8. Computed sensor e.m.f. at 650°C for different $k'_{F,II}$.

the e.m.f. curves lie between the curves shown in Fig. 5 for $k_{f,II} = 1.6$ and $k_{f,II} = 10^7$).

The ratio of adsorption rates of O_2 to that of CO, denoted by $r = (k^a_1/k^a_2)$, affects [1–5] the switch-point of the oxygen gas sensors. The expression relating the partial pressures of O_2 and CO at the switch-point, given by Eq. (9b) may be rewritten as

$$2P_{O2}/P_{CO} = [1 + (\kappa/k^a_1)(1 + k^d_1/k_D)] \times /[D_{O2}/D_{CO} + r(\kappa/k^a_1)]$$

The numerical value of (D_{O2}/D_{CO}) for binary diffusion is approximately 0.97 and in the present case $P_{O2} =$ 0.209. Then, using the parameter values mentioned above, one can rewrite the above equation in terms of the partial pressure of CO at the switch-point as

$$P_{CO} = 0.418(0.97 + r)/(2.1) \quad (14)$$

Assigning different values to r on electrodes I and II of the combustibles sensor amounts to (by Eq. (11)) subtraction of the e.m.f.s of two oxygen sensors which have different switch points. The authors define $r_I = k^a_{O2,I}/k^a_{CO,I}$, which is the ratio of adsorption rates of O_2 to that of CO on electrode I and assign it a constant value of 0.4 (i.e. $r_I = 0.4$). An oxygen sensor with $r_I = 0.4$ for its measurement electrode I would switch, by Eq. (14), at approximately $P_{CO} = 0.27$. Now the authors varied the ratio $r_{II} = k^a_{O2,II}/k^a_{CO,II}$ on electrode II, keeping the corresponding ratio on electrode I constant at 0.4 (i.e. $r_I = 0.4$). Fig. 6 depicts the combustibles sensor e.m.f. for a wide range of CO concentrations including stoichiometry (where $P_{CO} = 2P_{O2} = 0.418$). When r_{II} is equal to r_I, the e.m.f. has a small value (about 100 mV) for $P_{CO} < 0.3$ and abruptly drops close to zero for higher P_{CO} values. For $r_{II} > r_I$, the e.m.f. abruptly becomes large and positive at $P_{CO} =$ 0.3 and then suddenly drops close to zero at a larger P_{CO} value. The P_{CO} range of large positive e.m.f. expands as $r_{II}(> r_I)$ increases further. On the other hand, for $r_{II} < r_I$, the sensor e.m.f. suddenly becomes negative and large at a P_{CO} value less than 0.3 and then abruptly drops close to zero at $P_{CO} = 0.3$ as shown in Fig. 7. The P_{CO} range of large negative e.m.f. expands as $r_{II}(< r_I)$ decreases further. The overall behavior follows Eq. (11). As the switch-point corresponding to electrode II moves away from that for electrode I, the absolute value of the difference in the e.m.f.s remains large in the range of P_{CO} values lying between these two switch-points.

Finally, since the reaction rate constant k'_F affects both the high and low e.m.f. of the oxygen sensor, different values of k'_F on electrodes I and II of the combustibles sensor amounts to subtraction of the e.m.f.s of two oxygen sensors whose both high and low e.m.f. values are different. Fig. 8 shows the results of changing $k'_{F,II}$, keeping $k'_{F,I}$ constant at 10^5. Both the high and low e.m.f.s of the combustible sensor increase with decrease in the value of $k'_{F,II}$. The P_{CO} range of large positive e.m.f. expands as $k'_{F,II}$ decreases. Note that the large positive e.m.f. in Fig. 8 is due to the choice $r_I = 0.4$ and $r_{II} = 2.0$ so that $r_{II} > r_I$ (as in Fig. 6). One would have obtained large negative e.m.f. in Fig. 8 by choosing r_{II} such that $r_{II} < r_I$.

The examples depicted above illustrate the variety of results that can be obtained from the model. Thus, one can study the expected forms of the sensor response by changing the characteristics of the electrodes. Conversely, one can investigate the desired characteristics of the electrodes when the goal is to attain a specific form of the sensor response.

4. Conclusions

In conclusion, the authors have described an ab initio model for electrochemical metal oxide combustibles sensors which not only explains experimentally observed results but also can help in designing or optimizing this type of gas sensors. The authors plan to present a similar analysis for resistive sensors in a future publication.

References

[1] A.D. Brailsford, E.M. Logothetis, A steady-state diffusion model for solid-state gas sensors, Sens. Actuators 7 (1985) 39–67.

[2] A.D. Brailsford, M. Yussouff, E.M. Logothetis, Theory of gas sensors, Sens. Actuators B 13 (1993) 135–138.

[3] A.D. Brailsford, M. Yussouff, E.M. Logothetis, M. Shane, Steady-state model of a zirconia oxygen sensor in a simple gas mixture, Sens. Actuators B 24–25 (1995) 362–365.

[4] A.D. Brailsford, M. Yussouff, E.M. Logothetis, Theory of gas sensors: response of an electrochemical sensor to multi-component gas mixtures, Sens. Actuators B 34 (1996) 407–411.

[5] A.D. Brailsford, M. Yussouff, E.M. Logothetis, Steady state model of electrochemical gas sensors with multiple reactions, Sens. Actuators B 35–36 (1996) 392–397.
[6] H. Okamoto, H. Obayashi, T. Kudo, Carbon monoxide gas sensor made of stabilized zirconia, Solid State Ion. 1 (1980) 319–326.
[7] A. Vogel, G. Baier, V. Schuele, Non-Nernstian potentiometric zirconia sensors-screening of potential working electrode materials, Sens. Actuators B 15 (1993) 147–150.
[8] Handbook Chemistry and Physics, 58 ed., CRC Press, Boca Raton, FL, 1977, D-45.

Biographies

Alan Brailsford received his B.Sc., Ph.D. and D.Sc. degrees in mathematical physics from the University of Birmingham in 1953, 1956 and 1991, respectively. Dr. Brailsford has worked upon problems in the electron theory of metals, dislocation dynamics, radiation effects in metals and alloys and various topics in device physics. He is a fellow of the American Physical Society, ASM and of the Institute of Physics. He has recently retired as the manager of the Physics Department of the Ford Research Laboratory.

Mohammed Yussouff received his M.Sc. in 1963 from Delhi University and his Ph.D. in 1967 from the Indian Institute of Technology, Kanpur, where he was professor of physics until 1991. He worked in Juelich and Konstanz as a fellow of the Alexander von Humboldt Foundation. He is currently visiting professor at the Michigan State University and does research in the Physics and Physical Chemistry Department of General Motors Technical Center, Warren, MI. He has worked on channeling of ions, clusters, disordered systems, electronic structure of impurities in metals, foundations of quantum theory, ionic conductors, point defects, model of chemical sensors and the Theory of Freezing.

Eleftherios M. Logothetis received his B.S. degree in physics from the University of Athens, Greece, in 1959 and his M.S. and Ph.D. degrees in solid state physics from Cornell University in 1965 and 1967, respectively. He has been with the Ford Motor Company since 1967 and he is currently senior staff scientist in the Ford Research Laboratory. He is a fellow of the American Physical Society. His main research has been in the preparation and the electrical and optical properties of materials, solid state devices, in particular, chemical sensors.